A study of phase transition in the 2D Ising model using Markov Chain Monte Carlo simulation

Alessio Canclini, Filip von der Lippe
(Dated: November 20, 2022)

NB! Abstract here

I. INTRODUCTION

This article will explore temperature-dependent behavior in ferromagnetism using the two-dimensional **Ising model**. The main purpose of our simulations is to determine a numerical estimation of the **critical temperature** at which the system transitions from a magnetized to a non-magnetized phase. This is also called the Curie temperature. Past this point the magnetic spins are no longer aligned, causing the given ferromagnetic material to lose its magnetization.

With the Ising model we can easily model a magnetic materials' response to thermal energy. Magnet spins in the model have two states, either up or down. These can be flipped by energy input and each individual spin influences the total state of the system.

The Ising model is a widely studied model in statistical physics. Work on the model has shown to be useful for the analysis of several complex systems. Some examples are gasses sticking to solid surfaces or hemoglobin molecules that absorb oxygen. Additionally, when it comes to studies of phase transition, theoretical approaches such as mean field models can actually predict wrong behavior, further motivating the use of the Ising model.[1]

We will simulate the Ising model using a Markov Chain Monte Carlo (MCMC) approach. After testing our numerical method we will finally try to approximate the critical temperature for an infinite ($L = \infty$) 2D Isisng model. The analytical solution to this problem was found by Lars Onsager in 1944 [2]. Thus, our goal is not to necessarily find this temperature, but rather analyze how well our chosen MCMC approach can approximate such a complex problem.

To allow for reasonable runtimes for the larger computations our MCMC code is parallelized using OpenMP.

Section II will cover the theoretical background of the Ising model and MCMC method as well as some analytical solutions for code testing. More comprehensive derivations of the analytical values can be found in appendix A and B.

In section III we present results from our Ising model simulations. These cover comparison betwween analytic and numerical results, an analysis of burn-in time for a larger lattice size of $L = 20$ and finally an investigation of phase transitions.

A detailed discussion of the results and methods is then presented in section IV followed by a summary and concluding thoughts in section V.

II. METHODS

The square 2D lattices for our Ising model will have a length of L containing N spins with the relation $N = L^2$. Each spin s_i will have two possible states of

$$s_i = -1 \text{ or } s_i = +1.$$

The total spin state or **spin configuration** of a lattice will be represented as $\mathbf{s} = (s_1, s_2, ..., s_N)$. In its simplest form the total energy of the system is expressed as

$$E(\mathbf{s}) = -J \sum_{\langle kl \rangle}^{N} s_k s_l - \mathscr{B} \sum_{k}^{N} s_k.$$

Here $\mathscr{B}$ is an external magnetic field. Since we will be looking at the Ising model without an external magnetic field the equation will be simplified to

$$E(\mathbf{s}) = -J \sum_{\langle kl \rangle}^{N} s_k s_l, \tag{1}$$

where $\langle kl \rangle$ denotes the sum going over all *neighboring pairs* of spins avoiding double-counting. J is the **coupling constant** simply setting the energy associated with spin interactions. *Periodic boundary conditions* will be implemented allowing all spins to have four neighbors.

$$M(\mathbf{s}) = \sum_{i}^{N} s_i \tag{2}$$

is the magnetization of the entire system expressed as a sum over all spins. The energy per spin is

$$\epsilon(\mathbf{s}) = \frac{E(\mathbf{s})}{N} \tag{3}$$

and the magnetization per spin is given by

$$m(\mathbf{s}) = \frac{M(\mathbf{s})}{N}. \tag{4}$$

These values will be used to compare and analyze results.

$$\beta = \frac{1}{k_B T} \tag{5}$$

describes the "inverse temperature" with the systems' temperature T and the Boltzmann constant k_B.

$$Z = \sum_{\text{all possible } \mathbf{s}} e^{-\beta E(\mathbf{s})} \tag{6}$$

represents the partition function. This, the 'inverse temperature" and the total energy of the system appear in the *Boltzmann distribution*,

$$p(\mathbf{s}; T) = \frac{1}{Z} e^{-\beta E(\mathbf{s})}. \tag{7}$$

This will be the probability distribution used for random sampling in our Monte Carlo approach.

For comparison with early numerical implementations we will fist consider an analytical solution. The following table II summarizes all sixteen possible **spin configurations** of a 2×2 lattice with *periodic boundary conditions*.

Nr. of spins in state +1	Degeneracy	Total energy	Total magnetization
0	1	-8J	-4
1	4	0	-2
2	4	0	0
2	2	8J	0
3	4	0	2
4	1	-8J	4

TABLE I. Analytic values for the sixteen **spin configurations** of the 2×2 Ising model lattice.

Based on the values in table II we derive the specific analytical expressions for the 2×2 lattice case. The calculations of these analytic solutions can be found in appendix A and are used to test early versions of the code.

We will study properties of the system at equilibrium for different lattice sizes as a function of temperature T. The analysis will focus on four main properties. The mean energy (eq. 3), mean magnetization (eq. 4), specific heat capacity normalized to number of spins

$$C_V = \frac{1}{N} \frac{1}{k_B T^2} \left(\langle E^2 \rangle - \langle E \rangle^2 \right), \tag{8}$$

and the susceptibility normalized to number of spins

$$\chi = \frac{1}{N} \frac{1}{k_B T} \left(\langle M^2 \rangle - \langle |M| \rangle^2 \right). \tag{9}$$

Analytical solutions to these can also be found in appendix A.

Critical phenomena

The final goal for the MCMC simulations will be to approximate the critical temperature for an *infinite* ($L = \infty$) 2D Ising model. As mentioned in section I, the analytical solution for this was found by Lars Onsager. His result is

$$T_c(L = \infty) = \frac{2}{\ln\left(1 + \sqrt{2}\right)} J/k_B \approx 2.269 J/k_B.$$

For our approximation we will use the scaling relation

$$T_c(L) - T_c(L = \infty) = a L^{-1}. \tag{10}$$

Here a is constant. Theoretical background for this scaling realtion can be found in appendix C

Periodic boundary conditions

The Ising model simulations we will be implemented using periodic boundary conditions. This way, all spins will have four neighbors as seen in table II, also at the boundaries of the lattice.

$$\begin{array}{ccc} & \uparrow & \\ \uparrow & \uparrow & \uparrow \\ & \uparrow & \end{array}$$

FIG. 1. An example of a spin and its four neighbors. Here all five spins are in an up state (+1).

Markov chain Monte Carlo method

A Markov chain is a stok

The Metropolis algorithm

The algorithm generates a Markov chain

A flow chart of the Metropolis algorithm can be found in appendix D.

Optimization and parallelization

Periodic boundaries could be implemented using if-tests, but if-tests within loops can be slow. To make the code slightly more efficient we have chosen to write a `periodic` function using the modulo operator.

The Monte Carlo method will repeatedly require the Boltzmann factor $e^{-\beta \Delta E}$. The energy shift induced by flipping a single spin

$$\Delta E = E_{\text{after}} - E_{\text{before}} \tag{11}$$

can only take five possible values in a 2D-lattice of arbitrary size($L > 2$) This is shown in appendix B. These values are

$$\Delta E = 8J, 4J, 0, -4J, -8J. \tag{12}$$

To reduce computational cost we will avoid repeatedly calling the exponential function. This is done by precomputing the five possible Boltzmann factors in an array. Furthermore, the code is written such that it can be run parallelized. This allows us to run it on several threads using OpneMP to reduce runtimes.

III. RESULTS

To check the numerical implementation we compare analytical and numerical results for a 2×2 lattice case for $T = [0.5, 4.0] J/k_B$ in the following figures.

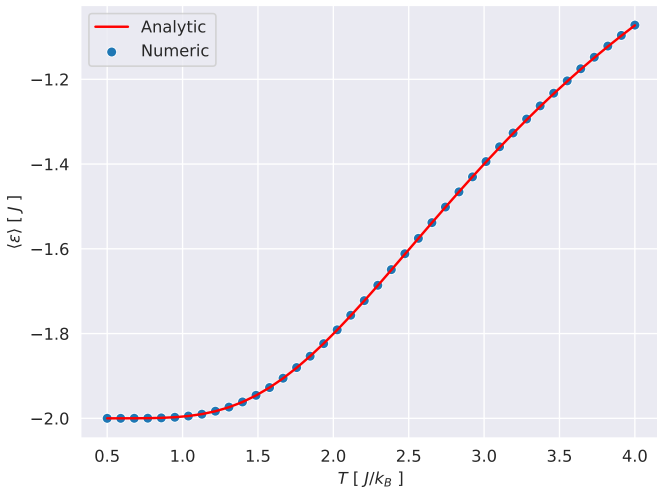

FIG. 2. Comparison of the red analytic and blue numeric results in a 2×2 lattice case. Here one sees the expectation value for the energy per spin ϵ plotted against different temperatures T. Numerical results shown are for 10^6 MC cycles.

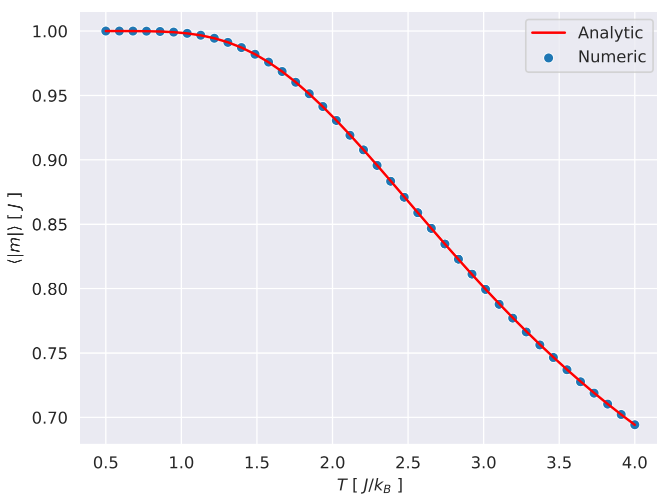

FIG. 3. Comparison of the red analytic and blue numeric results in a 2×2 lattice case. Here one sees the expectation value for the magnetization per spin m plotted against different temperatures T. Numerical results shown are for 10^6 MC cycles.

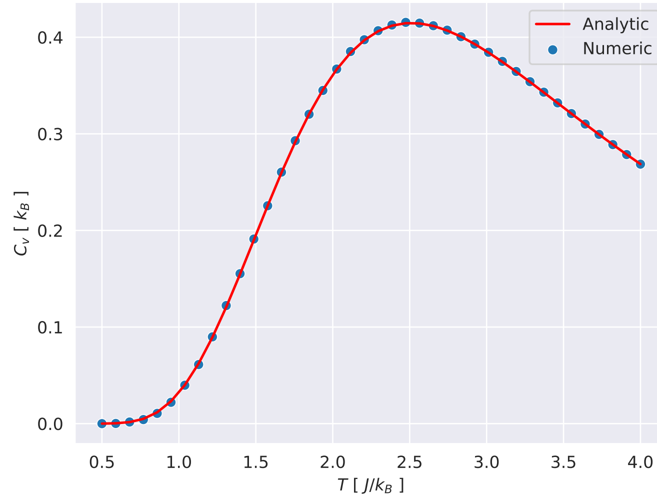

FIG. 4. Comparison of the red analytic and blue numeric results in a 2×2 lattice case. Here one sees the expectation value for the heat capacity C_V (normalized to number of spins) plotted against different temperatures T. Numerical results shown are for 10^6 MC cycles.

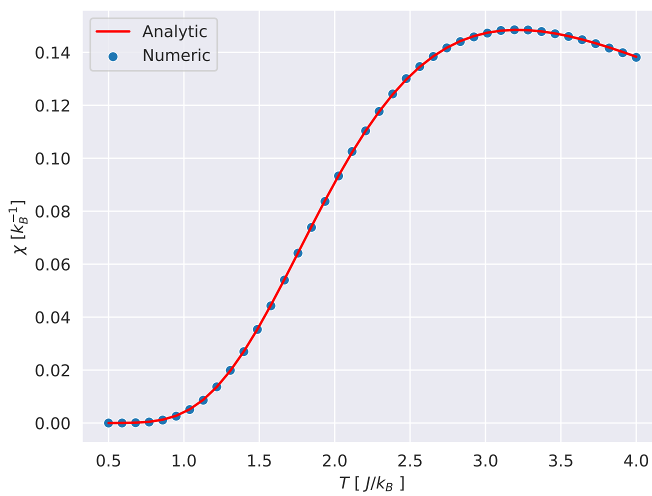

FIG. 5. Comparison of the red analytic and blue numeric results in a 2×2 lattice case. Here one sees the expectation value for the susceptibility χ (normalized to number of spins) plotted against different temperatures T. Numerical results shown are for 10^6 MC cycles.

Figures 2, 3, 4 and 5 show excellent agreement between numerical MCMC results and analytical results for a good range of temperatures shown.

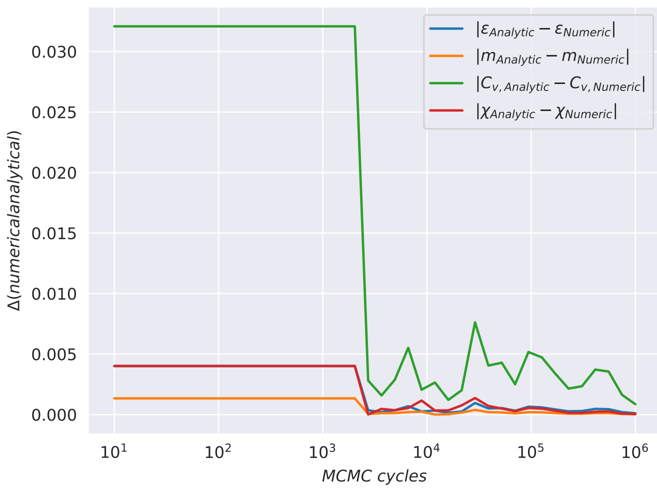

FIG. 6. The blue, yellow, green and red line show the change of the difference between numerical and analytical results as a function of MCMC cycles for $\langle\epsilon\rangle$, $\langle|m|\rangle$, C_V and χ respectively. In this case $L = 2$.

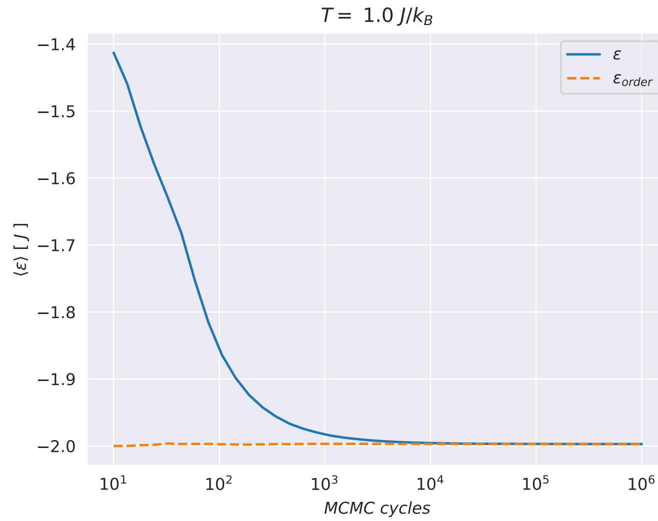

FIG. 7. Numerical approximation values for $\langle\epsilon\rangle$ against number of MCMC cycles for $T = 1.0 J/k_B$. The blue line shows the evolution from a random spin configuration whereas the orange line is for the case of an ordered spin configuration. Here $L = 20$.

In figure 6 one can see how the difference between numerical and analytical results decreases for increasing MCMC cycles. After about 10^5 cycles the numerical results stabilize and are in good agreement with the analytical result for a 2×2 lattice. Further computations will be run for 10^6 cycles to ensure precision since enough computational power is available.

This allows us to move on to more complex computations of larger lattice sizes. The next figures show results to study the **burn-in** time for our MCMC method for a 20×20 lattice. Results are shown for both a lattice with random spins and an ordered lattice with all spins starting in an up ($\uparrow$) state.

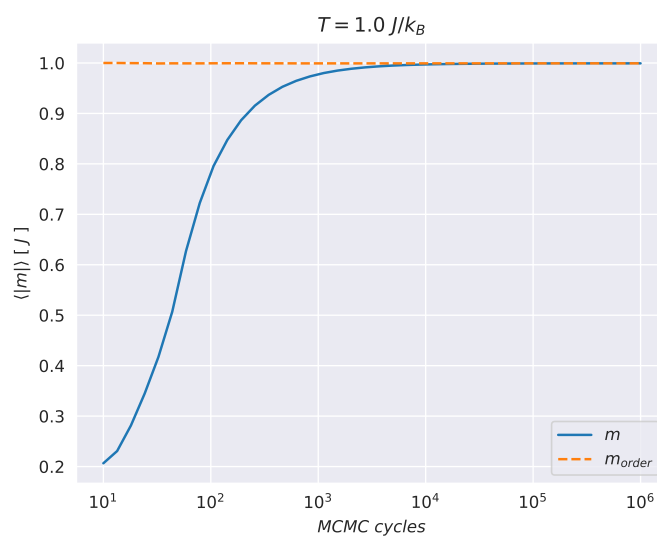

FIG. 8. Numerical approximation values for $\langle|m|\rangle$ against number of MCMC cycles for $T = 1.0 J/k_B$. The blue line shows the evolution from a random spin configuration whereas the orange line is for the case of an ordered spin configuration. Here $L = 20$.

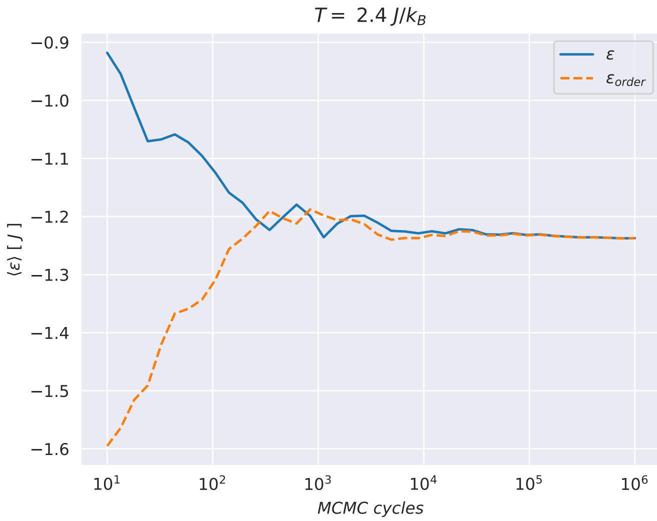

FIG. 9. Numerical approximation values for $\langle \epsilon \rangle$ against number of MCMC cycles for $T = 2.4 J/k_B$. The blue line shows the evolution from a random spin configuration whereas the orange line is for the case of an ordered spin configuration. Here $L = 20$.

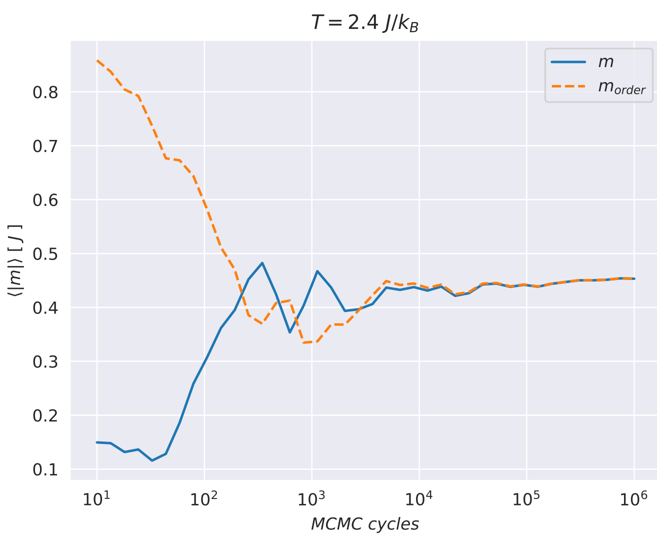

FIG. 10. Numerical approximation values for $\langle |m| \rangle$ against number of MCMC cycles for $T = 2.4 J/k_B$. The blue line shows the evolution from a random spin configuration whereas the orange line is for the case of an ordered spin configuration. Here $L = 20$.

Moving beyond expectation values we approximate the probability function $p_\epsilon(\epsilon; T)$ using MCMC samples. This is done for both $T = 1.0 J/k_B$ and $T = 2.4 J/k_B$.

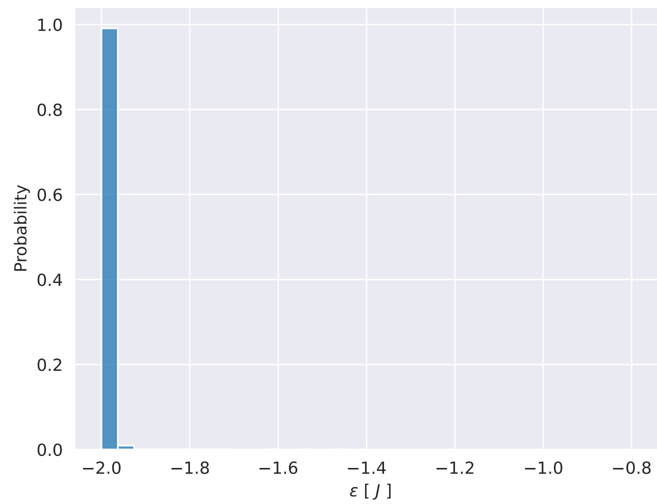

FIG. 11. Approximation of the probability function $p_\epsilon(\epsilon; T)$ for $L = 20$ and $T = 1.0 J/k_B$.

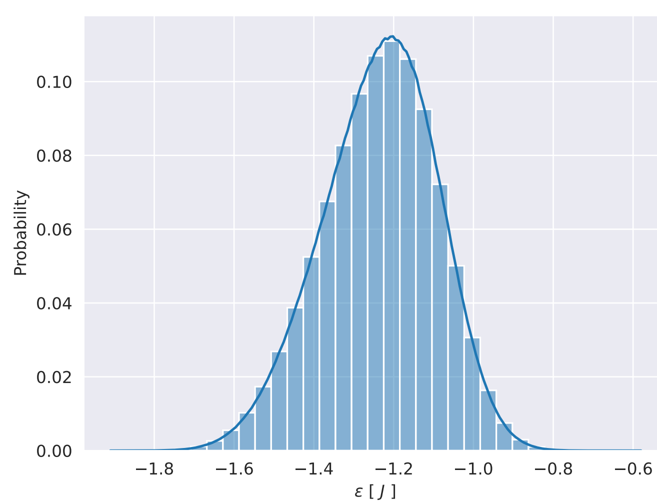

FIG. 12. Approximation of the probability function $p_\epsilon(\epsilon; T)$ for $L = 20$ and $T = 2.4 J/k_B$.

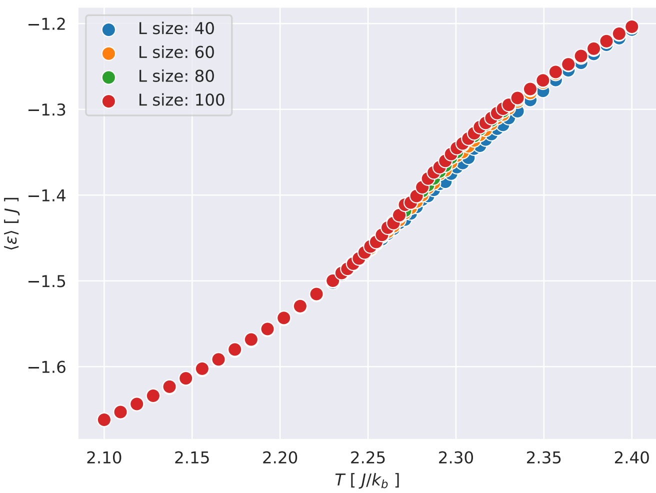

FIG. 13.

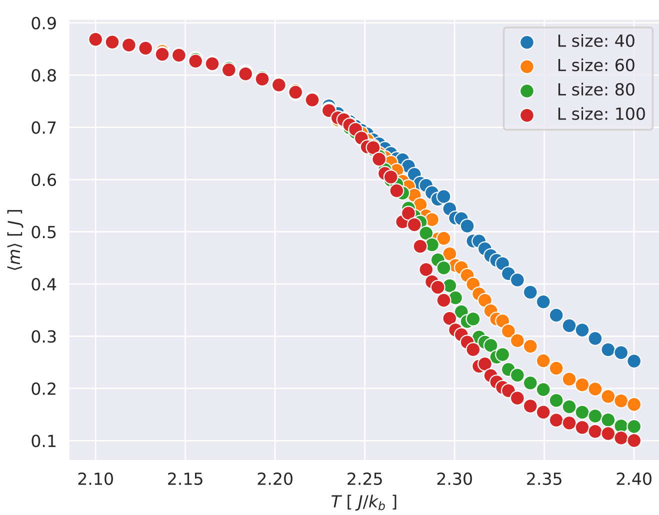

FIG. 14.

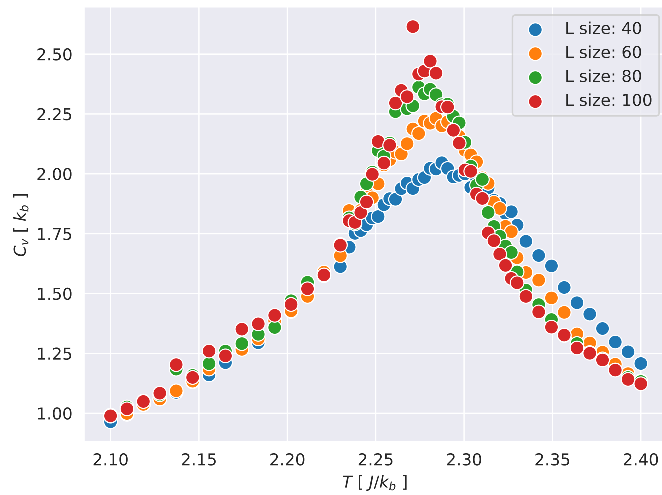

FIG. 15.

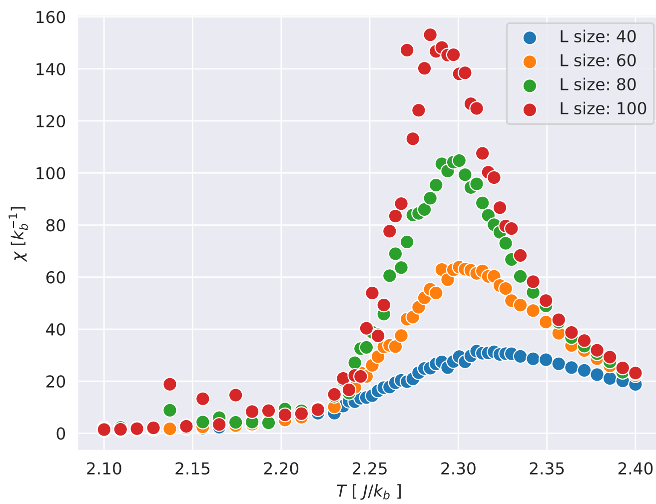

FIG. 16.

IV. DISCUSSION

Considering code optimization, we have chosen to parallelize the section of the code lopping over different temperatures and different numbers of cycles. This gives us time savings when we are plotting against these two variables, but not when running a single MCMC run. Another way of parallelizing the code would therefore be at the level of the MCMC "walkers" using several threads to execute multiple individual MCMC runs to finally combine the results. Whether this is more efficient for the computations that for example run over a range of different temperatures would require further investigation.

V. CONCLUSION

[1] M. Hjorth-Jensen, *Computational Physics* (Department of Physics, University of Oslo, 2015).
[2] UiO, "Project 4," .

Appendix A: Analytical solutions for a 2×2 lattice

For the case of a 2×2 lattice with $L = 2$ and $N = 4$ we have sixteen possible spin configurations show in table II. These values will be used for the analytic solutions. The specific partition function becomes

$$Z = \sum_{\text{all possible } \mathbf{s}} e^{-\beta E(\mathbf{s})} = 2e^{-\beta(-8J)} + 2e^{-\beta 8J} + 12e^0 = 2e^{\beta 8J} + 2e^{-\beta 8J} + 12 = 4(\cosh(8\beta J) + 3).$$

Additionally, we will calculate a few expectation values for which the general formula is given as

$$\langle A \rangle = \sum_s A_s p(s).$$

This is a sum over all spin states s_i. Here $p(s)$ is a chosen probability distribution, in our this case the Boltzmann distribution in eq. 7. For the energy we have

$$\begin{aligned}\langle E \rangle &= \sum_s E(\mathbf{s}) p(\mathbf{s}; T) = \frac{1}{Z}\sum_s E(\mathbf{s}) e^{-\beta E(\mathbf{s})} = \frac{1}{Z}\left(2\cdot(-8J)e^{\beta 8J} + 2\cdot 8Je^{-\beta 8J}\right) \\ &= \frac{1}{Z}\left(-16e^{\beta 8J} + 16e^{-\beta 8J}\right) = \frac{16J}{Z}\left(e^{-\beta 8J} - e^{\beta 8J}\right) = -\frac{32J\sinh(8J\beta)}{Z},\end{aligned}$$

$$\begin{aligned}\langle E^2 \rangle &= \sum_s E(\mathbf{s})^2 p(\mathbf{s}; T) = \frac{1}{Z}\sum_s E(\mathbf{s})^2 e^{-\beta E(\mathbf{s})} = \frac{1}{Z}\left(2\cdot(-8J)^2 e^{\beta 8J} + 2\cdot(8J)^2 e^{-\beta 8J}\right) \\ &= \frac{128J^2}{Z}\left(e^{-\beta 8J} + e^{\beta 8J}\right) = \frac{256J^2\cosh(8J\beta)}{Z},\end{aligned}$$

$$\langle \epsilon \rangle = \sum_s \epsilon_s p(\mathbf{s}; T) = \sum_s \frac{E(\mathbf{s})}{N} p(\mathbf{s}; T) = \frac{1}{N}\sum_s E(\mathbf{s}) p(\mathbf{s}; T) = \frac{\langle E \rangle}{4} = -\frac{8J\sinh(8J\beta)}{Z},$$

$$\langle \epsilon^2 \rangle = \sum_s \epsilon_s^2 p(\mathbf{s}; T) = \sum_s \left(\frac{E(\mathbf{s})}{N}\right)^2 p(\mathbf{s}; T) = \frac{1}{N^2}\sum_s E(\mathbf{s})^2 p(\mathbf{s}; T) = \frac{\langle E^2 \rangle}{16} = \frac{16J^2\cosh(8J\beta)}{Z}.$$

Then for the magnetization we have

$$\begin{aligned}\langle |M| \rangle &= \sum_s |M(\mathbf{s})| p(\mathbf{s}; T) = \frac{1}{Z}\sum_s |M(\mathbf{s})| e^{-\beta E(\mathbf{s})} = \frac{1}{Z}\left(|-4|e^{\beta 8J} + 4|-2|e^0 + 4|2|e^0 + |4|e^{\beta 8J}\right) \\ &= \frac{1}{Z}\left(4e^{\beta 8J} + 8 + 8 + 4e^{\beta 8J}\right) = \frac{8}{Z}\left(e^{\beta 8J} + 2\right),\end{aligned}$$

$$\begin{aligned}\langle M^2 \rangle &= \sum_s M(\mathbf{s})^2 p(\mathbf{s}; T) = \frac{1}{Z}\sum_s M(\mathbf{s})^2 e^{-\beta E(\mathbf{s})} = \frac{1}{Z}\left((-4)^2 e^{\beta 8J} + 4(-2)^2 e^0 + 4(2)^2 e^0 + (4)^2 e^{\beta 8J}\right) \\ &= \frac{1}{Z}\left(16e^{\beta 8J} + 16 + 16 + 16e^{\beta 8J}\right) = \frac{32}{Z}\left(e^{\beta 8J} + 1\right),\end{aligned}$$

$$\langle |m| \rangle = \sum_s |m(\mathbf{s})| p(\mathbf{s}; T) = \frac{1}{Z}\sum_s \left|\frac{M(\mathbf{s})}{N}\right| e^{-\beta E(\mathbf{s})} = \frac{\langle |M| \rangle}{4} = \frac{2}{Z}\left(e^{\beta 8J} + 2\right),$$

$$\langle m^2 \rangle = \sum_s m(\mathbf{s})^2 p(\mathbf{s}; T) = \frac{1}{Z}\sum_s \left(\frac{M(\mathbf{s})}{N}\right)^2 e^{-\beta E(\mathbf{s})} = \frac{\langle M^2 \rangle}{4^2} = \frac{\langle M^2 \rangle}{16} = \frac{2}{Z}\left(e^{\beta 8J} + 1\right).$$

Finally, we find analytical expressions for the specific heat capacity

$$C_V = \frac{1}{N}\frac{1}{k_B T^2}\left(\langle E^2 \rangle - \langle E \rangle^2\right) = \frac{1}{4}\frac{1}{k_B T^2}\left(\frac{256J^2\cosh(8J\beta)}{Z} - \left(-\frac{32J\sinh(8J\beta)}{Z}\right)^2\right),$$

and the susceptibility

$$\chi = \frac{1}{N}\frac{1}{k_B T}\left(\langle M^2\rangle - \langle |M|\rangle^2\right) = \frac{1}{4}\frac{1}{k_B T}\left(\frac{32}{Z}\left(e^{\beta 8J}+1\right) - \left(\frac{8}{Z}\left(e^{\beta 8J}+2\right)\right)^2\right).$$

Appendix B: Possible ΔE values

Considering a 2D lattice of arbitrary size ($L > 2$) and remembering that we are working with periodic boundary conditions, we can show that there are only a few possible values of ΔE. The calculation of ΔE between spin configurations will be limited to the flipping of a single spin. To find the possible energy differences we will look at a spin at a random position. This central spin will start in an up state(+1) and then be flipped (-1). We remind that $E(\mathbf{s}) = -J\sum_{\langle kl\rangle}^{4} s_k s_l$ and $\Delta E = E_{\text{after}} - E_{\text{before}}$.

$\begin{array}{ccc} & \uparrow & \\ \uparrow & \uparrow & \uparrow \\ & \uparrow & \end{array}$ has $E=-4J$, now flipping we have $\begin{array}{ccc} & \uparrow & \\ \uparrow & \downarrow & \uparrow \\ & \uparrow & \end{array}$ and $E = 4J$, resulting in $\Delta E = 8J$.

This can be show for the four remaining possible starting configurations as well.

$\begin{array}{ccc} & \uparrow & \\ \downarrow & \uparrow & \uparrow \\ & \uparrow & \end{array}$ has $E=-2J$. Flipping we have $\begin{array}{ccc} & \uparrow & \\ \downarrow & \downarrow & \uparrow \\ & \uparrow & \end{array}$ and $E = 2J$, resulting in $\Delta E = 4J$.

$\begin{array}{ccc} & \uparrow & \\ \downarrow & \uparrow & \uparrow \\ & \downarrow & \end{array}$ has $E=0$. Flipping we have $\begin{array}{ccc} & \uparrow & \\ \downarrow & \downarrow & \uparrow \\ & \downarrow & \end{array}$ and $E = 0$, resulting in $\Delta E = 0$.

$\begin{array}{ccc} & \uparrow & \\ \downarrow & \uparrow & \downarrow \\ & \downarrow & \end{array}$ has $E=2J$. Flipping we have $\begin{array}{ccc} & \uparrow & \\ \downarrow & \downarrow & \downarrow \\ & \downarrow & \end{array}$ and $E = -2J$, resulting in $\Delta E = -4J$.

$\begin{array}{ccc} & \downarrow & \\ \downarrow & \uparrow & \downarrow \\ & \downarrow & \end{array}$ has $E=4J$. Flipping we have $\begin{array}{ccc} & \downarrow & \\ \downarrow & \downarrow & \downarrow \\ & \downarrow & \end{array}$ and $E = -4J$, resulting in $\Delta E = -8J$.

The five possible values of the energy difference are thus, $\Delta E = 8J, 4J, 0, -4J, -8J$.

Appendix C: Theoretical background for critical phenomena

Power laws with so-called critical exponents describe how a physical system behaves when close to its critical point. For the Ising model this is close to its critical temperature. For temperatures T close to T_c the *infinite* 2D Ising model's mean magnetization, heat capacity and susceptibility behave as follows:

$$\begin{aligned}\langle|m|\rangle &\propto |T - T_c(L=\infty)|^{\beta},\\ C_V &\propto |T - T_c(L=\infty)|^{-\alpha},\\ \chi &\propto |T - T_c(L=\infty)|^{-\gamma}.\end{aligned}$$

Here $\beta = 1/8$, $\alpha = 0$ and $\gamma = 7/4$ are the critical exponents. We see that C_V and χ diverge close to T_c. The *correlation length*

$$\xi \propto |T - T_c(L=\infty)|^{-\nu} \tag{C1}$$

with $\nu = 1$ also diverges near T_c. For our finite system $\xi = L$ is the largest correlation length. Replacing for ξ in eq. C1 then leads to the scaling equation

$$T_c(L) - T_c(L=\infty) = aL^{-1}. \tag{C2}$$

Appendix D: Metropolis algorithm flow chart

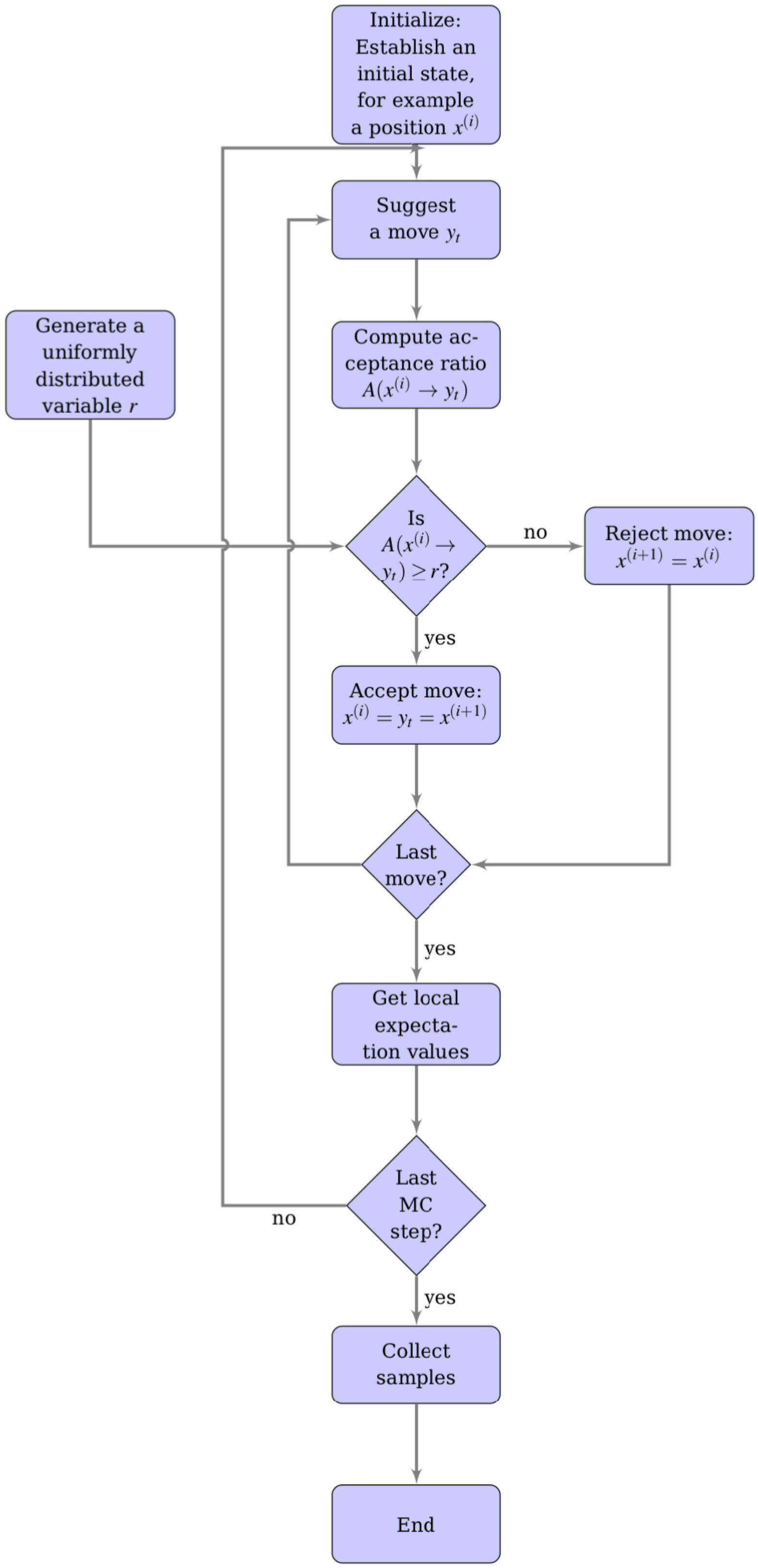

FIG. 17. Flowchart of the Metropolis algorithm taken from Computational Physics lecture notes [**?**].